

CASE DEPTH MEASUREMENT USING SURFACE ACOUSTIC WAVE VELOCITY DISPERSION

A. Safaeinili, A.D.W. McKie, and R.C. Addison, Jr.
Rockwell Science Center
1049 Camino Dos Rios
Thousand Oaks, CA 91360

INTRODUCTION

Case hardening is a metallurgical process typically to increase the fatigue and wear resistance of steel components. The *case* refers to the hardened layer that is formed in this process, and the depth of the case is critical to the components' performance. Currently, to inspect the quality of a batch of material that has gone through the hardening process, one or more of the parts are sectioned with an abrasive wheel, polished flat and the hardness profile measured using a microhardness indenter. This method of inspection can take several hours, often with the production line stopped, until the results are known. It does have the advantage of measuring directly the desired material properties but has the obvious disadvantages of costly manufacturing down-time, unnecessary scrapping of a production item and assumes that the material properties of other samples in the batch are similar to the one inspected. As a promising alternative approach, nondestructive inspection (NDI) permits a 100% inspection of the batch which is not economically viable using destructive inspection methods. Generally, NDI methods are based on inferring case depth indirectly through measuring electromagnetic or mechanical properties of the part using eddy current or ultrasonic probes [1-4]. Eddy current systems are commonly used for case depth measurements and are known to be reliable for many applications [4]. However, they lack sensitivity if the case depth is deep (e.g. greater than 5 mm in steel parts) and custom probes are required for inspection of components with different geometries.

Over the past three decades, many studies have demonstrated that a relationship between the elastic moduli of steel and its hardness exists. Also, ultrasonic case depth measurement techniques were proposed based on dispersion of Rayleigh wave

velocity [5]. More recent works show how case depth can be obtained from the group velocity dispersion [1,2]. The success of any of these techniques is critically dependent on the accuracy with which the SAW velocity dispersion can be measured in order to resolve changes in surface velocity of less than 1%. We have addressed this issue by first, measuring the phase velocity rather than group velocity, that is more difficult to define in practice at single frequencies; and secondly, we have developed a robust and precise technique to measure the SAW velocity using a scanning laser beam.

The three main obstacles in developing a SAW dispersion-based case depth inspection methods are: 1) existence of a strong correlation between hardness and the SAW phase velocity, 2) accurate measurement of surface velocity with accuracies of $\approx 0.1\%$, and 3) developing a robust and fast inversion algorithm for case depth parameter extraction. Papadakis [6] has measured ultrasonic velocities in three transformation products of steel indicating a 2% lower shear velocity for untempered martensite steel, which forms the hardened steel, versus pearlite or bainite which are mainly found in the core. He also indicated a 1.5% increase in shear wave velocity in tempered martensite versus untempered martensite. This increase in velocity in the tempered martensite is also observed in a recent measurement by Safaeinili et al. [7]. Inversion of SAW dispersion data has been addressed by Richardson [8] who uses a general inversion approach in which no *a priori* assumption about the case hardening profile is made. In order to achieve speed and robustness in inversion, we have specialized Richardson's solution to a model-based inversion algorithm with sufficient flexibility to match a variety of profiles that are likely to be observed in practice.

LASER-BASED ULTRASOUND SYSTEM

Figure 1 illustrates the experimental configuration for measurement of SAW phase velocity on steel axles and gear teeth using a laser-based ultrasound (LBU) system. A Q-switched Nd:YAG laser is directed at the axle surface and is focused to a line, resulting in propagation of surface waves normal to the illuminated line. LBU relies on the transient thermal expansion at a material surface that results from the sudden heating caused by illumination with a high power, short duration laser pulse [9]. Relief of the surface induced thermal stresses results in the propagation of elastic waves that emanate from the heated region. The incident generation laser energy was ≈ 5 mJ, that was sufficiently low to avoid material damage. The generated SAW propagates along the surface of the part where it is detected with a piezoelectric transducer (for axles) or a continuous wave (CW) argon-ion probe laser beam (for gear teeth). The phase modulated probe laser beam is collected and directed through a 0.5 m spherical Fabry-Pérot interferometer (SFPI) [10,11]. This interferometer converts the phase modulation of the probe laser, which is caused by the ultrasonically induced surface velocity, to an intensity modulation that is measured with a photodiode. Optical detection with a SFPI provides the most suitable means for noncontact detection from the rough surfaces typically encountered in industrial applications, such as the axle surface.

An LBU system has significant advantages over conventional contact piezoelectric techniques since it 1) eliminates the inconsistency problems encountered when using couplants, 2) provides spatially and temporally broadband generation and detection, hence removing the ambiguities associated with temporal and spatial transducer system response, 3) eliminates unnecessary propagation through contact wedges that can corrupt data, 4) provides access to small areas (e.g. gear teeth) that are not

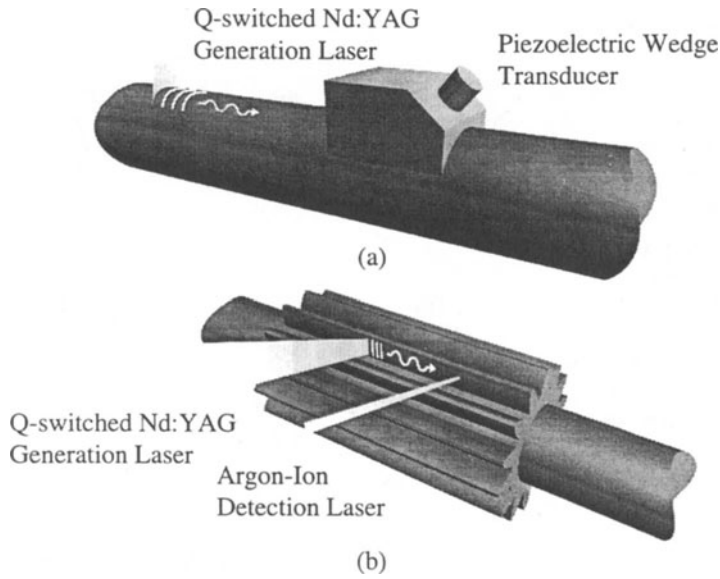


Figure 1. Experimental configuration for laser-based ultrasonic measurement of surface hardness in a) steel axle shaft and b) gear tooth. The generation laser is linearly scanned while the detection probe remains stationary.

accessible with relatively large and bulky conventional piezoelectric contact transducers and 5) has the ability to inspect parts with curved surfaces and complex geometry since the laser beam automatically conforms to the surface.

SAW PHASE VELOCITY MEASUREMENT

As shown in Figs. 1a and 1b, the generation laser beam is scanned with respect to a detection probe, resulting in acquisition of a series of spatially and temporally wideband waveforms $S(x_i, t)$. The series of waveforms are acquired at a number of equally spaced increments along the axle shaft. From the series of single shot ultrasonic waveforms, the phase velocity of the SAW can be estimated.

If no dispersion is present, the envelope of the wideband signal remains constant, with the measured ultrasonic propagation time delay remaining the same for equal steps in position. However, when the medium is dispersive, a single velocity cannot be defined for the envelope of the wideband signal since each frequency component of the signal travels with a different velocity. To separate these components, the time domain signals $S(x_i, t)$ are Fourier transformed to yield;

$$\hat{S}(x_i, \omega_j) = A(\omega_j) \exp[ip(x_i, \omega_j)] = \sum_{k=1}^n S(x_i, t_k) \exp[i\omega_j t_k] \Delta t \quad (1)$$

where, for a fixed frequency, the phase function $p(x_i, \omega_j) = \omega_j x_i / c(\omega_j)$ and $c(\omega_j)$ is the surface wave velocity for a given frequency ω_j . If time signals are acquired at sufficiently small steps (e.g. $\Delta x < \lambda_{min}/4$), the phase velocity can be measured directly from the slope of the unwrapped phase function [7].

Generally, this technique provides an accurate estimate of average phase velocity if the velocity variation is random and uncorrelated. This is due to redundant

measurements and a least square estimation of the slowness. Alternatively, very slow (i.e. on the order of the scan length) variations in the surface velocity in the direction of the scan may cause significant error in the phase velocity estimate. The existence of this condition is easily detected since the phase function $p(x, \omega)$ would have two or more different slopes corresponding to regions with different velocities. Furthermore, this method provides absolute phase velocity estimates for each frequency with an accuracy limited by the spatial resolution of the stepper motor controller without requiring the knowledge of source/receiver separation distance.

The least square estimate of the SAW phase velocity may be obtained in batch mode using a conventional line fitting algorithm, or alternatively in sequential mode using a recursive algorithm such as a Kalman filter [12]. For either approach, assuming a large number of acquired waveforms ($n > 10$), the error in the least square estimate of the SAW phase velocity, c , is given by [7]

$$\sigma_n^2 \approx \frac{3c^2\sigma_x^2}{n^3\Delta x^2} = \frac{3c^2\sigma_x^2}{nx_{max}^2} \quad (2)$$

The accuracy of this method is directly proportional to the scan length x_{max} and n , the number of waveforms acquired in the scan, and is inversely proportional to the stepper motor variance σ_x . For example, for a scan with $n = 30$ waveforms acquired over a 1 cm scan length with a stepper motor variance of less than $10 \mu m$, the accuracy for the SAW phase velocity estimate is $\approx 0.1\%$.

CORRELATION BETWEEN HARDNESS AND SAW VELOCITY

An important step in the ultrasonic determination of the case depth is obtaining a correlation between the SAW velocity and hardness. Surface hardening is achieved typically through a carburizing process or induction heat treatment [13]. In both processes, a number of parameters such as the amount or concentration of carbon, duration of treatment and temperature can be adjusted to control the surface hardness, its profile and the depth of the hardened case.

Although the hardening process involves phase transformations of steel, the variation in mechanical properties is due primarily to the macrostructural changes in steel during the heating and quenching process. For example, in the induction hardening process, the heat treatment transforms the steel from the pearlite phase, which is a body centered cubic phase of steel, into austenite that has a face centered cubic crystal structure. In the quenching stage, due to a rapid cooling of the heated part, the austenite transforms into martensite that is a supersaturated solution of carbon in a body centered tetragonal form of iron. The existence of interstitial carbon and the random orientation of martensite grains gives steel its hardness property and lower SAW velocity than in the pearlite phase. Furthermore, tempering can change the hardness and SAW velocity of the hardened layer while the crystal structure of the grains remains the same. The variation of SAW velocity is expected to be similar to that reported for the shear wave velocity. An example of such correlation for 1541H1 steel is shown in Fig. 2. To obtain this correlation, the SAW phase velocity for a set of 10 axles, with varying surface hardness ranging from 20 Rc to 58 Rc, was measured. The variation in hardness was achieved by subjecting a set of nominally identical axles, having a hardness of 58 Rc, through different degrees of tempering. The surface hardness was also measured independently using a microhardness indenter.

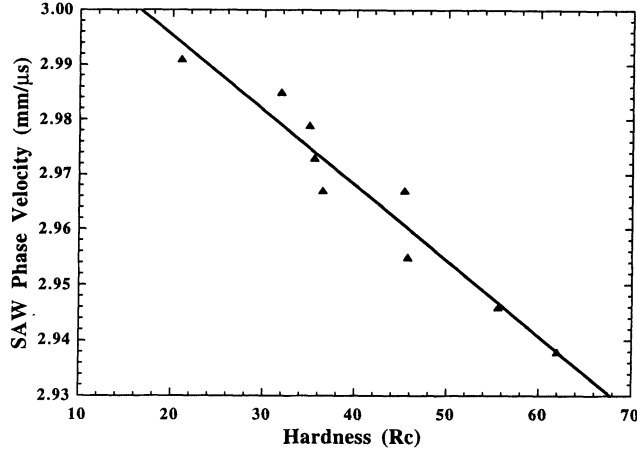


Figure 2. A comparison of surface hardness, measured with a microhardness indenter, and SAW phase velocity for segments of the steel truck axles. The results indicate a strong linear correlation.

ESTIMATION OF THE CASE DEPTH

The SAW velocity dispersion depends on the profile of the hardened region (case). This profile can be found by fitting a model to the experimental data. An accurate and computationally efficient model, based on a general perturbation analysis done by Auld [14] and then specialized by Thompson, is found in [8].

For an isotropic medium containing a layer with varying shear modulus, the change in the Rayleigh velocity can be written as

$$\Delta v = -\frac{(vk_1k_3^l)^2\mu}{P} \int_0^\infty (Exp[-k_3^l x_3] - Exp[-k_3^t x_3])^2 f(x_3) dx_3 \quad (3)$$

where v is the Rayleigh velocity, P is the total unperturbed propagating energy per unit width, k_1 and $k_3^{l,t}$ are the projections of the wavenumbers in the directions parallel and normal to the propagation direction respectively, x_3 is the depth parameter (direction normal to the surface), and $f()$ is the profile function for the variation in shear modulus μ . The expression for P can be found in [8].

The parameters in the profile function $f()$ can be found by an optimization algorithm that involves multiple calculations of Δv . The speed of convergence to a solution is related directly to the speed of calculation for Δv . To reduce the computation time for calculation of Δv , the profile function $f(x)$ is expressed in terms of a piecewise linear function as

$$f(x) = \sum_{i=1}^m [f_i + \frac{\Delta f_i}{\Delta x_i}(x - x_i)] \Psi(x_i, \Delta x_i) \quad (4)$$

where m is the number of segments, Δx_i is the segment width, $f_i = f(x_i)$ (note that $f(x)$ may be discontinuous, i.e. $f(x_i) \neq f(x_{i-1}) + \Delta x_i$) and

$$\Psi(x_i, \Delta x_i) = \begin{cases} 1 & x_i \leq x < x_i + \Delta x_i \\ 0 & \text{otherwise} \end{cases} \quad (5)$$

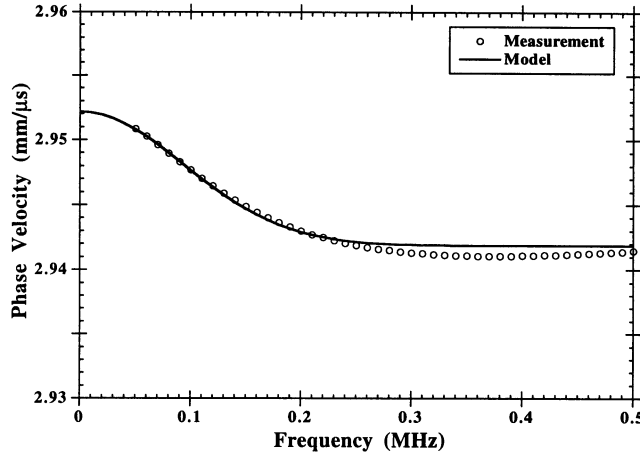


Figure 3. Experimental and theoretical SAW phase velocity dispersion curves for a 48 mm diameter axle with a case depth of 11 mm.

By substituting the expression for $f(x)$, Equation (3) can be evaluated as

$$\Delta v = -\frac{(vk_1k_3^l)^2\mu}{P} \sum_{i=1}^N I(2k_3^l; d_i, \Delta d_i) - 2I((k_3^l + k_3^t); d_i, \Delta d_i) + I(2k_3^t; d_i, \Delta d_i) \quad (6)$$

where d_i is the depth of the layer i from the surface, Δd_i is the thickness for layer i and function $I()$ can be written as

$$I(\alpha; d, \Delta d) = \frac{\exp(-\alpha d_i)}{\alpha} v_i (1 - \exp(-\alpha \Delta d_i)) + \frac{\Delta v_i}{\Delta d_i} [(d_i + \frac{1}{\alpha})(1 - \exp(-\alpha \Delta d_i)) - \Delta d_i \exp(-\alpha \Delta d_i)] \quad (7)$$

Note that for $\Delta v_i = 0$ the model simplifies to the case of the profile function with a step discontinuity. Most cases of interest in this work can be modeled using only two terms in the profile function $f()$ (i.e. $N=2$). If higher accuracy is needed, N can be increased accordingly.

The simplest model that belongs to this family of functions is composed of a single homogeneous layer on a half-space. For this case, there are three unknown parameters: 1) Rayleigh wave velocity parameter in the layer material, 2) Rayleigh wave velocity parameter in the substrate, 3) the layer thickness parameter (or case depth). An example of the SAW dispersion curve obtained for an axle with a nominal case depth of 12 mm is shown in Fig. 3. The SAW is generated by a spatially and temporally broadband Nd:YAG laser pulse and is detected by a piezoelectric transducer which is coupled to the axle using a wedge. The transducer has a center frequency of 500 kHz and is 25 mm in diameter. The generation laser beam is scanned over a 57 mm line along the axis of the axle in 0.57 mm steps. The experimental dispersion curve is obtained using the processing scheme outlined above. The model calculation shown in this figure is based on a single uniform hardened layer on a uniform core. The SAW velocity of the hardened layer is known from the

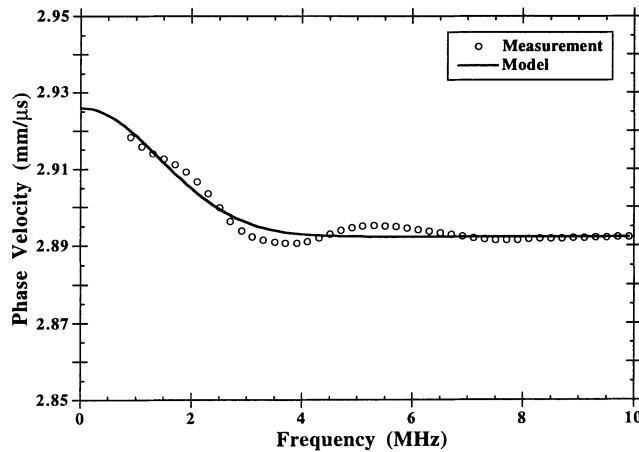


Figure 4. Experimental and theoretical SAW phase velocity dispersion curves for a gear tooth. Measurements were obtained using an LBU system as shown in Fig. 1b.

high frequency region of the dispersion curve where most of the SAW energy is confined in the hardened layer. Consequently, only the SAW velocity of the core and the case depth parameter remain to be found. The estimated case depth for this axle was 10.7 mm, which is within 4% of the average indenter measurement of 11.1 mm.

Similar measurements were performed for a 50 mm long gear tooth where a Q-switched Nd:YAG laser was again used for ultrasonic wave generation and an argon-ion probe laser, in conjunction with a SFPI, was used for the detection of the SAW. The SFPI is most sensitive at 4 MHz but yields useful data extending from 0.5 MHz to 20 MHz. The experimental and theoretical dispersion curves are shown in Fig. 4. The fit indicates a 0.7 mm effective case depth based on a single layer model. Unlike the axles that are induction hardened and have sharp transition regions between the hardened layer and the core, the hardness in carburized gears has a slow linear transition from the surface to the core. Consequently, the effective hardness, which corresponds to the width of a layer having a constant hardness of the surface, must be calibrated to obtain the depth at which hardness falls below 50 Rc.

In interpreting the case depth parameters obtained from the dispersion curve, one has to realize that the accuracy is dependent on the existence of a strong correlation between hardness and SAW velocity. Consequently, for each application where metallurgy is different, this correlation needs to be verified. Furthermore, additional calibration may be needed to compensate for the inaccuracies of the theoretical model.

SUMMARY

This work presents a method for measuring the depth of the hardened layer (case) on steel parts based on velocity dispersion of SAW. For this purpose, experimental and data processing techniques for precise measurement of SAW phase velocity were developed. The spatial and temporal wideband nature of the LBU system allows SAW velocity measurements to be performed with accuracies of $\approx 0.1\%$. Also, a linear correlation between surface hardness and SAW phase velocity for induction hardened steel was presented. The linear correlation between hardness

and the SAW velocity can be used to estimate of the effective case depth based on the SAW velocity dispersion. This method was successfully used to measure the effective case depth of hardened gear teeth and axles. The next step is to improve the accuracy of the model by considering metallurgical factors such as existence of a transition layer between the hardened surface and the core. This is especially important in estimation of case depth in axles where the case depth is as deep as 12 mm.

ACKNOWLEDGEMENTS

This work was supported by the Rockwell Commercial Research and Development funds through Rockwell Automotive Heavy Vehicle Systems Division. The authors thank D. Donegan, S. Foster and J. Khoury at Rockwell Heavy Vehicle Systems for providing the axle samples for this work and M. Calabrese, at Science Center, for making the hardness measurements and performing the metallographic studies.

REFERENCES

1. A. Abbate, S.C. Schroeder, B.E. Knight, F. Yee and J. Frankel, *Review of Progress in Quantitative Nondestructive Evaluation*, Vol. 15A (Eds. Thompson, D.O. and Chimenti, D.E.) (Plenum Press, New York, 1996) p.585 .
2. G. Gordon and B.R. Tittmann, *Review of Progress in Quantitative Nondestructive Evaluation*, Vol. 15, Eds. D.O. Thompson and D.E. Chimenti, Plenum Press, New York, (1996) p. 1597.
3. M. Rosen *Materials Analysis by Ultrasonics*, Ed. A. Vary, Noyes Data Corp. , 79 (1987).
4. C.H. Stephen and H.L. Chesney, *Materials Evaluation*, Vol. 42, (1984) p. 1612.
5. B.R. Tittmann and R.B. Thompson, in *Proc. of the 9th Symp. on NDT Tech*, SWRI, San Antonio, TX, p. 20, 1973.
6. E.P. Papadakis, *J. Appl. Phys.*, Vol. 35(5), (1964) p. 1474.
7. A. Safaeinili, A.D.W. McKie, and R. C. Addison, Jr., to appear in *Material Research Bulletin*, Vol. 21, No. 10, 1996.
8. J.M. Richardson, *Journal of Appl. Physics*, Vol. 48(2), pp. 498-512, 1977.
9. C.B. Scruby and L.E. Drain, *Laser Ultrasonics - Techniques and Applications* (Adam Hilger, New York 1990).
10. J.M. Vaughan, *The Fabry-Pérot Interferometer: History, Theory, Practice and Applications* (Adam Hilger, New York 1989).
11. J.-P. Monchalain and R. Heon, *Materials Evaluation* Vol. 44, 1231 (1986).
12. A. Gelb ed., *Applied Optimal Estimation*, (M.I.T. Press, Cambridge 1988) p. 105.
13. T. Lyman ed., *ASM Metals Handbook* Vol. 2, 8th Edition, (1964) p. 93.
14. B. A. Auld, *Acoustic Fields and Waves in Solids, II*, (Krieger Publishing Company, Malabar, Florida 1990), Ch. 12.